THE JOURNAL OF PHYSICAL CHEMISTRY A

Article

pubs.acs.org/JPCA

Experimental and Theoretical Kinetics for the $H_2O^+ + H_2/D_2 \rightarrow H_3O^+/H_2DO^+ + H/D$ Reactions: Observation of the Rotational Effect in the Temperature Dependence

Shaun G. Ard,[†] Anyang Li,[‡] Oscar Martinez, Jr.,[†] Nicholas S. Shuman,[†] Albert A. Viggiano,*[,†,‡] and Hua Guo*[,‡]

[†]Space Vehicle Directorate, Air Force Research Laboratory, Kirtland AFB, Albuquerque, New Mexico 87117, United States

[‡]Department of Chemistry and Chemical Biology, University of New Mexico, Albuquerque, New Mexico 87131, United States

ABSTRACT: Thermal rate coefficients for the title reactions computed using a quasi-classical trajectory method on an accurate global potential energy surface fitted to ~81,000 high-level ab initio points are compared with experimental values measured between 100 and 600 K using a variable temperature selected ion flow tube instrument. Excellent agreement is found across the entire temperature range, showing a subtle, but unusual temperature dependence of the rate coefficients. For both reactions the temperature dependence has a maximum around 350 K, which is a result of H_2O^+ rotations increasing the reactivity, while kinetic energy is decreasing the reactivity. A strong isotope effect is found, although the calculations slightly overestimate the kinetic isotope effect. The good experiment−theory agreement not only validates the accuracy of the potential energy surface but also provides more accurate kinetic data over a large temperature range.

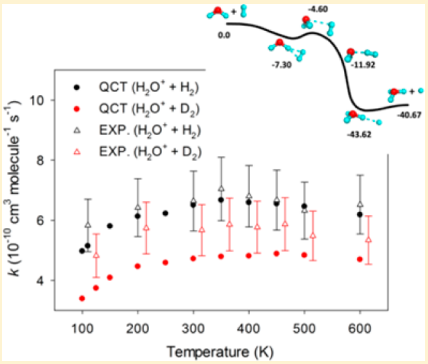

I. INTRODUCTION

The reaction between the water molecular ion and molecular hydrogen is a key step in the formation of hydroxyl radical and water molecules in the interstellar medium.[1−3] Indeed, H_2O^+ has recently been detected in many different regions of outer space, thanks to the Herschel space observatory.[4−6] As a result, the accurate determination of the rate coefficients for these reactions at low temperatures is desired for astrochemical models. So far, however, the rate coefficients have mostly been measured near room temperature and the experimental data contain large uncertainties.[7−14]

In addition, the title reactions have been used to investigate mode specificity in reaction dynamics thanks to advances in laser technology that allow selective population of single quantum states.[15,16] The effects of translational, rotational, and vibrational excitations on reactivity have been systematically investigated.[17−19] With collision energies (E_c) ranging from thermal to 10 eV, the measured absolute integral reaction cross sections (ICSs) were found to decay monotonically with E_c, implying an exothermic, barrierless reaction pathway. The most surprising result of the state-resolved experiments is the observation of a large enhancement of the reactivity by exciting the H_2O^+ rotational degrees of freedom, particularly at low E_c values. These experimental results are unexpected, as internal excitations in reactants usually have little impact on the reactivity of complex-forming reactions.[20] Only a few systems have been observed to have strong effects from rotation on reactivity; while most exhibit simpler behavior depending on total energy.[21,22] In the reaction of O^+ with HD there is a strong preference for forming OH^+ compared to OD^+, which depends on rotational motion. This branching has been attributed to the center of mass and center of polarizability being different, thereby affecting which end of the HD molecule "hits" O^+ more frequently.[23−25] Increased rotational motion decreases the effect. For the reaction of Kr^+ with HCl, a distinct rotational effect has never been explained.[26] Clearly, such effects pose a challenge for theoretical interpretation.

To understand the kinetics and reaction dynamics of the title reaction, we have systematically investigated the reaction pathway using a high level ab initio method,[19] culminating with a full-dimensional global potential energy surface (PES).[27] The PES was fit to ~81,000 points at the UCCSD(T)-F12/AVTZ level[28,29] using the accurate permutation invariant polynomial neural network (PIP-NN) method.[30,31] The PIP-NN PES, which is invariant with respect to permutation of identical atoms in the system, provides an accurate analytical representation of the high-level ab initio points, with a root-mean-square error (RMSE) of merely 15 cm^{-1}. Consistent with experimental observations, the reaction path was found to be barrierless. However, it has a submerged saddle point that forms a bottleneck for the reaction. With the help of the recently proposed Sudden Vector Projection model,[32−34,35] it was shown that the surprising rotational enhancement observed in recent experiments is due to the strong coupling of the H_2O^+ rotational degrees of freedom with the reaction coordinate at the submerged saddle point.[27] In addition, the rate coefficients

Received: October 15, 2014
Revised: November 14, 2014
Published: November 14, 2014

were computed on the PES using a quasi-classical trajectory (QCT) method, and the agreement with the available experimental data at room temperature was satisfactory, although the latter was rather scattered. In addition, a weak temperature dependence was predicted by the QCT calculations at other temperatures.

In order to examine the accuracy of these theoretical predictions, confirm the rotational effects, and establish the temperature dependence of the rate coefficients, experimental measurements of the rate coefficients have been performed using a variable temperature selected ion flow tube (SIFT) instrument for both the $H_2O^+ + H_2$ and $H_2O^+ + D_2$ reactions. This work compares the newly measured kinetic data with an expanded set of theoretical values spanning the temperature range from 100 to 600 K.

II. EXPERIMENTAL SECTION

All measurements were performed on the Air Force Research Laboratory's variable temperature selected ion flow tube instrument, which has been described in detail elsewhere.[26] Briefly, H_2O^+ ions are created using electron impact ionization on vapor from deionized water. The ions are extracted and injected into a quadrupole mass filter for exclusive selection of H_2O^+. Mass-selected ions are focused and subsequently introduced into a laminar flow tube via a Venturi inlet, where $\sim 10^4$ to 10^5 collisions with a He buffer gas thermalize the ions and carry them downstream. The temperature of the flow tube is variable over a large range by using pulsed liquid nitrogen (100−220 K), recirculating methanol chillers (220−300 K), or resistive heating devices (300−700 K). The pressure in the flow tube is variable over a small range and was generally 0.35 Torr at room temperature, varying only slightly with temperature. The neutral reagent (H_2 and D_2) is added 59 cm upstream from the end of the flow tube, resulting in typical reaction times on the order of 4 ms, dependent on helium buffer flow (varied from 10 to 13 std. L min^{-1}) and temperature.

After traveling the length of the flow tube, the core of the flow is sampled through a truncated nosecone with a 2 mm aperture. After the nosecone, primary and product ions are guided by a lens stack to a quadrupole mass filter for analysis and are subsequently detected using an electron multiplier operated in counting mode. Rate coefficients are derived by monitoring the decay of the primary ion as a function of the neutral reagent flow. Linear decays in the parent ion signal on a semilogarithmic scale were observed over 2−3 orders of magnitude allowing for derivation of the rate coefficient. Measurements were made from 100 to 600 K and a temperature dependency of the rate coefficients determined. Errors in the rate coefficients are estimated to be ±25% absolute and ±15% relative to each other.[26]

III. THEORY

Thermal rate coefficients for the $H_2O^+ + H_2$ and $H_2O^+ + D_2$ reactions were computed on the recently developed full-dimensional PES,[27] using the standard QCT method implemented in VENUS.[36,37] At each specific temperature, T, the initial ro-vibrational energies of the two reactants and relative translational energy, E_{rel}, were sampled according to the Boltzmann distribution. The maximal impact parameter (b_{max}) was determined using small batches of trajectories with trial values at each temperature. The rate coefficient at T was calculated as follows:

$$k(T) = \left(\frac{8k_BT}{\pi\mu}\right)^{1/2} \pi b_{max}{}^2 \frac{N_r}{N_t} \quad (1)$$

where μ is the translational reduced mass, k_B is the Boltzmann constant, and N_r and N_t are the reactive and total trajectory numbers, respectively. The standard error is given by $\Delta = ((N_t - N_r)/(N_tN_r))^{1/2}$. Trajectories were initiated with a reactant separation of 10.0 Å and terminated when products reached a separation of 6.0 Å or when reactants are separated by 10.0 Å for nonreactive trajectories. A total of 50,000 trajectories were used at each temperature, resulting in statistical errors on the order of 1%. During propagation, the gradient of the PES was obtained numerically by a central-difference algorithm. The propagation time step was selected to be 0.02 fs, which conserves energy better than 0.04 kcal/mol for most trajectories. Trajectories that failed to conserve energy to 0.04 kcal/mol or were nonreactive after 4.0 ps were discarded. We did not attempt to analyze the internal state distributions of the products, but the zero-point energy issues are not expected to be a problem thanks to the large exoergicity of the reaction.

IV. RESULTS AND DISCUSSION

The schematic PES for this system is given in Figure 1. As discussed before, the overall reaction pathway is barrierless, but

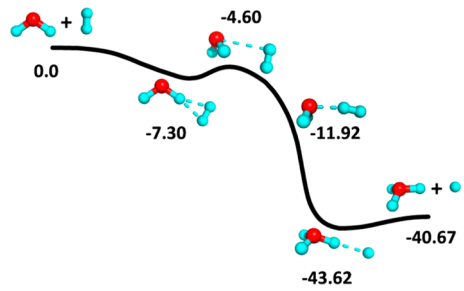

Figure 1. Schematic depiction of the PES along the reaction coordinate for the reaction of $H_2O^+ + H_2$. The geometries and energies (in kcal/mol) of stationary points are provided.

there is a submerged barrier 4.6 kcal mol^{-1} below the reactants near the entrance channel, which provides a reaction bottleneck.[27] Beyond the saddle point, there is a shallow well corresponding to the H_4O^+ complex 43.6 kcal mol^{-1} below reactants, and the reaction is highly exothermic (ΔE = 40.7 kcal mol^{-1}).

The room temperature rate coefficients for the reactions of H_2O^+ with both H_2 and D_2 are shown in Table 1, along with previously reported values. Both reactions are found to react at roughly half their Langevin collision rates, with the D_2 reaction being slightly more efficient. The current measurement for the reaction with H_2 agrees well with previous measurements by Rakshit and Warneck[13] and Kim et al.,[10] but only just agrees with the previous SIFT measurement by Jones et al.[14] within the combined uncertainties. The current rate coefficient for the reaction with D_2 falls between the two previously reported values,[7,9] though both of these were determined by techniques considered less reliable by today's standards. Experimentally, only H_2DO^+ product from the reaction with D_2 is observed, with an upper limit of 5% for the HD_2O^+ channel. This is consistent with the trajectory calculations, which only find 4 out of 50,000 trajectories lead to HD_2O^+ product. Furthermore, this is also consistent with the expected lifetime of the shallow

dx.doi.org/10.1021/jp510399v | J. Phys. Chem. A 2014, 118, 11485−11489

Table 1. Measured Rate Coefficients[a]

	$H_2O^+ + H_2$		$H_2O^+ + D_2$	
temp (K)	k (10^{-10} cm^3 s^{-1})	$k/k_{Langevin}$	k (10^{-10} cm^3 s^{-1})	$k/k_{Langevin}$
110	5.8	0.39	4.8	0.44
200	6.4	0.43	5.7	0.52
300	6.6[b]	0.44	5.5[c]	0.50
350	7.0	0.47	5.9	0.53
400	6.8	0.45	5.8	0.52
500	6.7	0.44	5.9	0.53
600	6.3	0.42	5.5	0.50

[a]The absolute error of the current work is estimated at ±25% with relative uncertainties of ±15%. [b]Lit. values include 4.0,[13] 8.3,[14] 6.4,[12] 8.3,[11] 6.1,[10] and 14.0[8] in units of 10^{-10} cm^3 s^{-1}. [c]Lit. values include 4.0[9] and 8.0[7] in units of 10^{-10} cm^3 s^{-1}.

intermediate well leading to products being too short to allow for a statistical distribution of the products.

The temperature dependences of both reaction rate coefficients are shown in Figure 2. The experimental rate

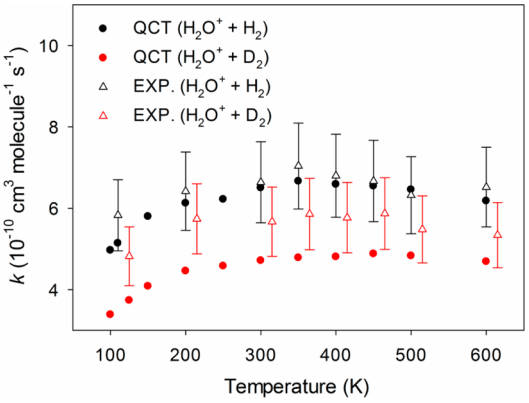

Figure 2. Comparison of the measured and computed rate coefficients for the $H_2O^+ + H_2$ and $H_2O^+ + D_2$ reactions, with 15% relative error bars shown. The experimental data for D_2 have been offset for clarity.

coefficients for H_2 appear to have a very slight maximum at 350 K; however, only the fastest and slowest values are actually outside the relative error when comparing individual points. A more sophisticated statistical analysis involving all low or high temperature points is more conclusive. Assuming that the data follow a smooth trend (such as a power law, which is common for ion−molecule reactions) and that the experimental errors represent normal distributions, it is highly likely (>95%) that the data between 110 and 350 K follow a positive temperature dependence and quite likely (>80%) that the data from 350 to 600 K follow a negative temperature dependence. Figure 3 shows the probability distribution of the experimental temperature dependences under this assumption. Indeed, the data in those two regions are independently well described by either a power law or exponential fit, while the full set of data is not. Similar evaluation of the $H_2O^+ + D_2$ data yields a similarly high likelihood for a maximum around 350 K. In total, the experimental data show the likely presence of a hump in the rate coefficient as a function of temperature outside of uncertainty. This conclusion is also strongly supported by the theoretical calculations, which show nearly identical trends, also peaking at ∼350 K. Therefore, it does appear that the rate coefficient increases slightly at temperatures below ∼350 K and decreases at higher temperatures.

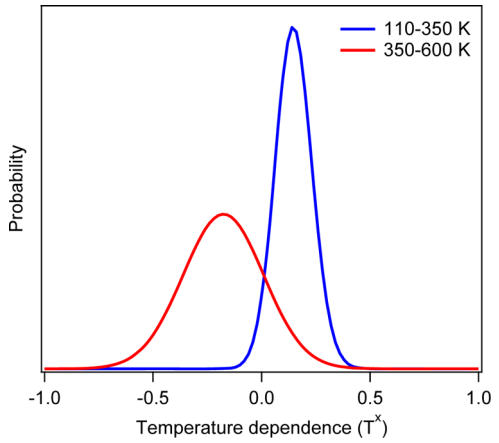

Figure 3. Probability distribution of the temperature dependence of the experimental rate coefficients from the present work over the indicated temperature ranges, assuming the data is described by a power law.

These unusual temperature dependences confirm work by the Ng group,[17−19] which showed that, at low J, H_2O^+ rotations increase reactivity, while kinetic energy decreases the rate coefficients. Extrapolation of the Ng group's cross sections to lower energies and integration to thermal rate coefficients suggests somewhat higher values than the current measurements and computational results. However, exact comparison is not possible because the rotational state-resolved measurements do not include all states contributing significantly to the present thermal distributions. The rotational dependence reported by Ng and co-workers can qualitatively explain the observed temperature dependence. At 100 K, ∼35% of the H_2O^+ molecules will be in $J = 0$ and another ∼30% in $J = 1$. These two states are the slowest in the beam experiments. These values drop to 26 and 23% at 300 K and 15 and 14% at 600 K. Thus, the slight increase in rate coefficients we see at low temperature is the rotational enhancement on the rate coefficient winning out over the negative dependence on kinetic energy. The decrease at higher temperatures is small. The results of Ng and colleagues showed the rotational effect decreasing with higher kinetic energy, and this effect will decrease the temperature dependence. Their kinetic energy dependences are slightly more negative than the Langevin prediction, which corresponds to a T^0 dependence in the rate coefficient, in agreement with the present $T^{-0.1}$ or $T^{-0.2}$ dependence. A slight negative temperature dependence in the rate coefficient is consistent with a submerged barrier, which, as in this case, leads to a long-lived intermediate (i.e., $H_2O^+\cdots H_2$). As the energy increases, the unimolecular rate coefficient for dissociation back to reactants through the loose entrance channel increases faster than the rate coefficient to products over the tighter transition state, resulting in a decreasing rate coefficient.[27] This implies that H_2 rotations have little effect on reactivity, consistent with observations from the trajectory calculations. The rotational enhancement has been attributed to the fact that the lowest energy pathway has the H_2 approaching the H end of H_2O^+ due to long-range electrostatic forces, while the reaction proceeds through a complex with H_2 adjacent to the O. Rotations prevent "locking" onto the wrong site. This effect diminishes as the molecules approach faster.

The D_2 rate coefficients are lower than those for H_2, in part because the collisional rate coefficient is lower. While the

dx.doi.org/10.1021/jp510399v | J. Phys. Chem. A 2014, 118, 11485−11489

agreement between the experiment and calculation for $H_2O^+ + H_2$ is exceptional, the agreement for $H_2O^+ + D_2$ is merely good, reproducing the trends very well, but differing in absolute magnitude by 15−25%, at the edge of experimental error. This level of the theory−experiment agreement provides strong evidence in support of the accuracy of the PES. The weak temperature dependence is consistent with the barrierless pathway for these reactions.

In Figure 4, the kinetic isotope effect (KIE) is displayed as a function of the temperature. The $H_2O^+ + D_2$ reaction has a lower reactivity (ratio >1) throughout the entire temperature range, although the D_2 reaction has a lower collisional rate coefficient (1.1×10^{-9} cm^3 s^{-1} vs 1.5×10^{-9} cm^3 s^{-1})[38,39] and is actually more efficient. The collisional rate coefficients were determined by the parametrization according to Su and Chesnavich,[38] which is identical in this case to the Langevin rate since higher order terms (e.g., quadrupole moment or dipole moment of the ion) are not of importance under the present conditions. The agreement between theory and experiment is at the edge of our uncertainty. Interestingly, given the narrow range, both the theoretical and experimental data have similar wiggles, possibly fortuitously. This trend in the isotope effect is consistent with that observed in the integral cross section measurements by Ng and co-workers.[19] Indeed, the $H_2O^+ + H_2$ reaction was found to be more reactive at low collision energies than the $H_2O^+ + D_2$ reaction, although the cross sections are similar above 1.0 eV. The large isotope effect of the cross section at low collision energies is consistent with KIE in the rate coefficients. The origin of the greater efficiency for D_2 is still not entirely clear, but it presumably stems from the lower zero point energy associated with the heavier deuterium atoms.

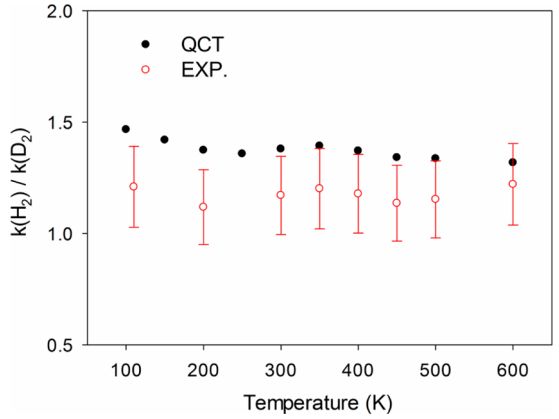

Figure 4. Comparison of the measured and computed kinetic isotope effects for the $H_2O^+ + H_2$ and $H_2O^+ + D_2$ reactions with 15% relative error bars shown.

V. SUMMARY

In this work, we report experimental measurements of the rate coefficients for the $H_2O^+ + H_2/D_2$ reactions using a selected ion flow tube instrument. The new data not only provide more accurate rate coefficients at room temperature but also temperature dependences. The magnitude and the weak temperature dependence of the measured rate coefficients is consistent with the barrierless reaction pathway, which is slightly inhibited by a submerged barrier. A maximum in the rate coefficient observed in both the experiment and calculations is unusual. Apparently, this interesting temperature dependence arises from the combination of a rotational enhancement of reactivity at low J levels, with a general decrease in efficiency at higher energy common to reactions with a submerged barrier such as this. The results confirm the rotational dependence on H_2O^+ found in beam experiments.

These newly measured experimental data are in very good agreement with theoretical predictions made using QCT on an accurate global PES. The level of agreement for the $H_2O^+ + H_2$ reaction is particularly impressive, with theory reproducing the subtle but intricate temperature dependence. The absolute agreement is less satisfactory for the $H_2O^+ + D_2$ reaction, resulting in some errors in the KIE. Given that the QCT used to compute the rate coefficients is incapable of capturing all quantum effects, such a level of agreement is quite remarkable and provides convincing evidence for the accuracy of the PES. It is unfortunate that neither the current experimental approach nor theoretical method can be trusted to extend the temperature dependence to an astrochemically relevant range (10−50 K), given the nontrivial temperature dependence observed over the present range. However, future quantum mechanical determination of the rate coefficients on the same PES might supply the much needed kinetic data at low temperatures.

AUTHOR INFORMATION

Corresponding Authors

*E-mail: afrl.rvborgmailbox@kirtland.af.mil.
*E-mail: hguo@unm.edu.

Notes

The authors declare no competing financial interest.

ACKNOWLEDGMENTS

This work is supported by the Department of Energy Office of Science, Office of Basic Energy Research (DE-FG02-05ER15694 to H.G.) and by the Air Force Office of Scientific Research (AFOSR-2303EP to A.A.V.). O.M. acknowledges the National Research Council. S.G.A. acknowledges the support of Boston College Institute of Scientific Research. H.G. thanks Cheuk Ng for numerous stimulating discussions.

REFERENCES

(1) Herbst, E.; Klemperer, W. Formation and Depletion of Molecules in Dense Interstellar Clouds. *Astrophys. J.* **1973**, *185*, 505−533.
(2) Watson, W. D. Interstellar Chemistry. *Acc. Chem. Res.* **1977**, *10*, 221−226.
(3) Hollenbach, D.; Kaufman, M. J.; Neufeld, D.; Wolfire, M.; Goicoechea, J. R. The Chemistry of Interstellar OH^+, H_2O^+, and H_3O^+: Inferrring the Cosmic-Ray Ionization Rates from Observations of Molecular Ions. *Astrophys. J.* **2012**, *754*, 105−127.
(4) Neufeld, D. A.; Goicoechea, J. R.; Sonnentrucker, P.; Black, J. H.; Pearson, J.; Yu, S.; Phillips, T. G.; Lis, D. C.; De Luca, M.; Herbst, E.; et al. Herschel/Hifi Observations of Interstellar OH^+ and H_2O^+ Towards W49N: A Probe of Diffuse Clouds with a Small Molecular Fraction. *Astron. Astrophys.* **2010**, *521*, L10.
(5) Gerin, M.; De Luca, M.; Black, J.; Goicoechea, J. R.; Herbst, E.; Neufeld, D. A.; Falgarone, E.; Godard, B.; Pearson, J. C.; Lis, D. C.; et al. Interstellar OH^+, H_2O^+ and H_3O^+ Along the Sight-Line to G10.6−0.4. *Astron. Astrophys.* **2010**, *518*, L110.
(6) Gonzalez-Alfonso, E.; Fischer, J.; Bruderer, S.; Muller, H. S. P.; Gracia-Carpio, J.; Sturm, E.; Lutz, D.; Poglitsch, A.; Feuchtgruber, H.; Veilleux, S.; et al. Excited OH^+, H_2O^+ and H_3O^+ in NGC 4418 and Arp 220. *Astron. Astrophys.* **2013**, *550*, A25.

(7) Kubose, D. A.; Hamill, W. H. Velocity Dependence of Ion−Molecule Reaction Cross Sections in a Mass Spectrometer. *J. Am. Chem. Soc.* **1963**, *85*, 125−127.
(8) Fehsenfeld, F. C.; Schmeltekopf, A. L.; Ferguson, E. E. Thermal-Energy Ion-Neutral Reaction Rates 7. Some Hydrogen-Atom Abstraction Reactions. *J. Chem. Phys.* **1967**, *46*, 2802−2808.
(9) Harrison, A. G.; Thynne, J. C. J. Concurrent Ion−Molecule Reactions 4. Reactions in Mixtures of Ammonia and Water with Deuterium and Methane. *Trans. Faraday Soc.* **1968**, *64*, 945−953.
(10) Kim, J. K.; Theard, L. P.; Huntress, W. T. ICR Studies of Some Hydrogen-Atom Abstraction Reaction: $X^+ + H_2 \rightarrow XH^+ + H$. *J. Chem. Phys.* **1975**, *62*, 45−52.
(11) Dotan, I.; Lindinger, W.; Rowe, B.; Fahey, D. W.; Fehsenfeld, F. C.; Albritton, D. L. Rate Constants for the Reactions of H_2O^+ with NO_2, O_2, NO, C_2H_4, CO, CH_4, and H_2 Measured at Relative Kinetic Energies 0.04 - 2 eV. *Chem. Phys. Lett.* **1980**, *72*, 67−70.
(12) Rakshit, A. B.; Warneck, P. Reactions of CO_2^+, $CO_2CO_2^+$ and H_2O^+ Ions with Various Neutral Molecules. *J. Chem. Soc., Faraday Trans. II* **1980**, *76*, 1084−1092.
(13) Rakshit, A. B.; Warneck, P. A Drift Chamber Study of the Reaction $ArH^+ + H_2 \rightarrow H_3^+ + Ar$ and Related Reactions. *J. Chem. Phys.* **1981**, *74*, 2853−2859.
(14) Jones, J. D. C.; Birkinshaw, K.; Twiddy, N. D. Rate Coefficients and Product Ion Distributions for the Reactions of OH^+ and H_2O^+ with N_2, O_2, NO, N_2O, Xe, CO, CO_2, H_2S and H_2 at 300 K. *Chem. Phys. Lett.* **1981**, *77*, 484−488.
(15) Ng, C.-Y. State-Selected and State-to-State Ion-Molecular Reaction Dynamics by Photoionization and Differential Reactivity Methods. *Adv. Chem. Phys.* **1992**, *82*, 401−500.
(16) Ng, C.-Y. State-Selected and State-to-State Ion−Molecule Reaction Dynamics. *J. Phys. Chem. A* **2002**, *106*, 5953−5966.
(17) Xu, Y.; Xiong, B.; Chang, Y. C.; Ng, C. Y. Communication: Rovibrationally Selected Absolute Total Cross Sections for the Reaction $H_2O^+(X^2B_1; v_1^+v_2^+v_3^+=000; N^+K_a^+K_c^+) + D_2$: Observation of the Rotational Enhancmeent Effect. *J. Chem. Phys.* **2012**, *137*, 241101.
(18) Xu, Y.; Xiong, B.; Chang, Y. C.; Ng, C. Y. The Translational, Rotational, and Vibrational Energy Effects on the Chemical Reactivity of Water Cation $H_2O^+(X^2B_1)$ in the Collision with Deuterium Molecule D_2. *J. Chem. Phys.* **2013**, *139*, 024203.
(19) Li, A.; Li, Y.; Guo, H.; Lau, K.-C.; Xu, Y.; Xiong, B.; Chang, Y.-C.; Ng, C. Y. Communication: The Origin of Rotational Enhancement Effect for the Reaction of $H_2O^+ + H_2$ (D_2). *J. Chem. Phys.* **2014**, *140*, 011102.
(20) Guo, H. Quantum Dynamics of Complex-Forming Bimolecular Reactions. *Int. Rev. Phys. Chem.* **2012**, *31*, 1−68.
(21) Viggiano, A. A.; Morris, R. A. Rotational and Vibrational Energy Effects on Ion−Molecule Reactivity as Studied by the VT-SIFDT Technique. *J. Phys. Chem.* **1996**, *100*, 19227−19240.
(22) Green, R. J.; Qian, J.; Kim, H.-T.; Anderson, S. L. Hydride Abstraction by NO^+ from Ethanol: Effects of Collision Energy and Ion Rotational State. *J. Chem. Phys.* **2000**, *113*, 3002−3010.
(23) Dateo, C. E.; Clary, D. C. Isotopic Branching Ratio for the O^+ + HD Reaction. *J. Chem. Soc., Faraday Trans. II* **1989**, *85*, 1685−1696.
(24) Sunderlin, L. S.; Armentrout, P. B. Temperature Dependence of the Reaction of O^+ with HD. *Chem. Phys. Lett.* **1990**, *167*, 188−192.
(25) Viggiano, A. A.; Vandoren, J. M.; Morris, R. A.; Williamson, J. S.; Mundis, P. L.; Paulson, J. F.; Dateo, C. E. Rotational Temperature Dependence of the Branching Ratio for the Reaction of O^+ with HD. *J. Chem. Phys.* **1991**, *95*, 8120−8123.
(26) Viggiano, A. A.; Morris, R. A.; Dale, F.; Paulson, J. F.; Giles, K.; Smith, D.; Su, T. Kinetic Energy, Temperature, and Derived Rotational Temperature Dependences for the Reactions of $Kr^+(^2P_{3/2})$ and Ar^+ with HCl. *J. Chem. Phys.* **1990**, *93*, 1149−1157.
(27) Li, A.; Guo, H. A Nine-Dimensional Ab Initio Global Potential Energy Surface for the $H_2O^+ + H_2 \rightarrow H_3O^+ + H$ Reaction. *J. Chem. Phys.* **2014**, *140*, 224313.
(28) Adler, T. B.; Knizia, G.; Werner, H.-J. A Simple and Efficient CCSD(T)-F12 Approximation. *J. Chem. Phys.* **2007**, *127*, 221106.
(29) Knizia, G.; Adler, T. B.; Werner, H.-J. Simplified CCSD(T)-F12 Methods: Theory and Benchmarks. *J. Chem. Phys.* **2009**, *130*, 054104.
(30) Jiang, B.; Guo, H. Permutation Invariant Polynomial Neural Network Approach to Fitting Potential Energy Surfaces. *J. Chem. Phys.* **2013**, *139*, 054112.
(31) Li, J.; Jiang, B.; Guo, H. Permutation Invariant Polynomial Neural Network Approach to Fitting Potential Energy Surfaces. II. Four-Atomic Systems. *J. Chem. Phys.* **2013**, *139*, 204103.
(32) Jiang, B.; Guo, H. Relative Efficacy of Vibrational vs. Translational Excitation in Promoting Atom-Diatom Reactivity: Rigorous Examination of Polanyi's Rules and Proposition of Sudden Vector Projection (SVP) Model. *J. Chem. Phys.* **2013**, *138*, 234104.
(33) Jiang, B.; Guo, H. Control of Mode/Bond Selectivity and Product Energy Disposal by the Transition State: The X + H_2O (X = H, F, $O(^3P)$, and Cl) Reactions. *J. Am. Chem. Soc.* **2013**, *135*, 15251−15256.
(34) Jiang, B.; Li, J.; Guo, H. Effects of Reactant Rotational Excitation on Reactivity: Perspectives from the Sudden Limit. *J. Chem. Phys.* **2014**, *140*, 034112.
(35) Guo, H.; Jiang, B. The Sudden Vector Projection Model: Mode Specificity and Bond Selectivity Made Easy. *Acc. Chem. Res.* **2014**, in press (DOI: 10.1021/ar500350f).
(36) Hase, W. L.; Duchovic, R. J.; Hu, X.; Komornicki, A.; Lim, K. F.; Lu, D.-H.; Peslherbe, G. H.; Swamy, K. N.; Linde, S. R. V.; Varandas, A.; et al. VENUS96: A General Chemical Dynamics Computer Program. *Quantum Chem. Program Exch. Bull.* **1996**, *16*, 671.
(37) Hase, W. L. Classical Trajectory Simulations: Initial Conditions. In *Encyclopedia of Computational Chemistry*; Alinger, N. L., Ed.; Wiley: New York, 1998; Vol. *1*, pp 399−402.
(38) Su, T.; Chesnavich, W. J. Parametrization of the Ion−Polar Molecule Collision Rate Constant by Trajectory Calculations. *J. Chem. Phys.* **1982**, *76*, 5183−5185.
(39) Maergoiz, A. I.; Nikitin, E. E.; Troe, J.; Ushakov, V. G. Classical Trajectory and Adiabatic Channel Study of the Transition from Adiabatic to Sudden Capture Dynamics. II. Ion−Quadrupole Capture. *J. Chem. Phys.* **1996**, *105*, 6270−6276.